

Gait Graph Optimization: Generate Variable Gaits from One Base Gait for Lower-limb Rehabilitation Exoskeleton Robots

Lei Zhang¹, Weihai Chen¹, Yuan Chai², Jianhua Wang¹, Jianbin Zhang¹

Abstract—The most concentrated application of lower-limb rehabilitation exoskeleton (LLE) robot is that it can help paraplegics “re-walk”. However, “walking” in daily life is more than just walking on flat ground with fixed gait. This paper focuses on variable gaits generation for LLE robot to adapt complex walking environment. Different from traditional gaits generator for biped robot, the generated gaits for LLEs should be comfortable to patients. Inspired by the pose graph optimization algorithm in SLAM, we propose a graph-based gait generation algorithm called gait graph optimization (GGO) to generate variable, functional and comfortable gaits from one base gait collected from healthy individuals to adapt the walking environment. Variants of walking problem, e.g., stride adjustment, obstacle avoidance, and stair ascent and descent, help verify the proposed approach in simulation and experimentation. We open source our implementation³.

I. INTRODUCTION

Many patients have lost their motor functions in their lower limbs because of diseases like cerebral apoplexy [1] or accident. Recently, developing LLE robots to assist locomotion for paraplegics has been a growing interest task of industry as LLEs have been applied successfully in many applications, including strength augmentation [2] and rehabilitation [3]. Until now, there has been significant progress for this task including Ekso, Fourier X1, ReWalk [4], HAL [5] and WAPL [6]. All of these robots can help patients walk smoothly at a flat ground with fixed gait. However, sometimes patients need to adjust their gait for obstacle avoidance [7] or stair ascent and descent [8]. It is the main issue to develop effective approaches for adapting complex walking environment so that LLEs can be used in life.

Considering that paraplegics can hardly provide walking power by themselves, the control strategy of LLEs developed for paraplegic is trajectory tracking control in general. Therefore, the reference joint trajectory for lower-limb, which we call “gait” is quite essential. Traditionally, LLEs simply collect gaits from healthy individuals as the reference joint trajectory, such as Mina [9] and Fourier X1. However, this strategy would break down when facing with dimensions obstacles. For different users and different environments, the gait of every walk cycle can be diversely. Unfortunately, It

is impossible to record all the gaits from healthy individuals walking on every condition. Hence, an algorithm that can generate functional and variable gaits is quite essential.

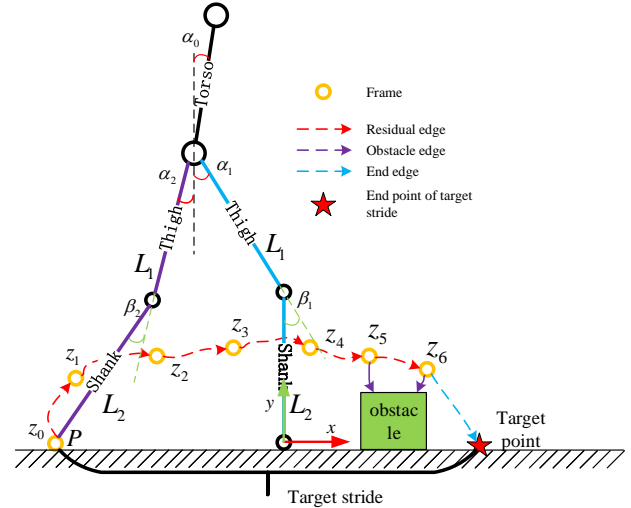


Fig. 1: Simplified model of LLE robot.

One may face with three kinds of conditions that need to adjust his gait: 1) Adjust his stride to step over a pit. 2) Adjust his gait for obstacle avoidance. 3) Adjust his gait for stair ascent and descent. Although all these conditions have been researched in robot arms [10][11] or biped robots [12][13], these approaches can not be applied in LLEs directly. These methods did not consider whether the gaits are comfortable for paraplegics. Jatsun et al. proposed a strategy to avoid obstacles for LLE [7]. However, this article only considered the trajectory of the endpoint of swing leg to avoid the obstacle, and the joint angle was solved by the inverse kinematics, which indicates that the comfort of generated gaits can not be guaranteed. Until now, significant progress has been made in the stair ascent and descent strategies for LLE [14][15]. However, these two works did not discuss gaits generated online. Sergey et al. proposed an optimization-based algorithm [8] for stair ascent, and the joint trajectory was solved by inverse kinematics, which is similar to [7]. Recently, Zhong et al. did a great work for stair ascent and descent with LLE [16], which could generate smooth gait. However, the height of stairs is estimated by the first step, which indicates that this algorithm will not work for stairs with different heights of stair edges. Without the prior knowledge of the stair’s height, the height of the first step should be set high enough to step over an uncertain stair. Moreover, without the referenced gait of a healthy person,

This work is supported by the National Nature Science Foundation under Grant 61773042, 51675018, 61573047.

¹Lei Zhang, Weihai Chen, Jianhua Wang, Jianbin Zhang are with the School of Automation science and Electrical Engineering, Beihang University, Beijing, China. e-mail: leizhangbuaa@163.com, whchenbuaa@126.com

²Yuan Chai is with the School of Astronautics, National Key Laboratory of Aerospace Flight Dynamics, Northwestern Polytechnical University,

³<https://github.com/leilegele1/GGO.CERES.git>

the comfort of gait can not be guaranteed.

Actually, the basic geometry of obstacles and stairs can be estimated by depth cameras and lidars [17]-[19]. Now we assume that the geometry of obstacle and stair is obtained, and there exists one gait collected from healthy individuals walking on flat ground, which we call it "base gait". Generally speaking, the base gait is comfortable for patients. If variable gaits can be generated from the base gait with minor modification, the comfort of generated gaits can be guaranteed. Inspired by the pose graph optimization [20], we propose gait graph optimization, which can generate gaits from the base gait with minor modification. Besides, we will show how to generate gaits with the proposed algorithm for stride adjustment, obstacle avoidance, and stair ascent and descent in detail.

II. RELATED WORK

Pose graph optimization [20] (PGO) is a state-of-the-art formulation for loop closure problem in SLAM. In the SLAM framework, one odometry is adopted to estimate the transformation between two adjacent frames. While there exists minor gaussian noise in the estimated transformations, the little error on transforms will accumulate to a large error on the final estimated pose. A loop closure detector (LCD) is utilized to detect the close-loop of two frames and estimate the transform between them. In the pose graph, the nodes are estimated poses of frames, the weak edges are the estimated transformations from odometry, and the strong edge is the estimated transformations from LCD. Finally, the Gaussian noise on the weak edges can be eliminated with the guidance of strong edges by solving the graph. The main idea of PGO is to utilize the transformation of close-loop as prior knowledge to eliminate the minor noise between every two adjacent frames. What inspires us is that if we add errors to the strong edge deliberately, we can also use PGO to add minor and uniform errors to each weak edge to generate a totally different trajectory. Compared with real trajectory, every transformation between two adjacent frames in the generated trajectory is quite similar, but the whole trajectories are totally different. This idea can be transferred to generate variable gaits for LLEs from one base gait.

III. KINEMATICS MODEL & BASE GAIT

A. Kinematic model of LLE

The kinematic model of LLE robot is simplified as a five-link model, as shown in Fig.1, where the blue leg and purple leg denote the supporting leg and swinging leg. A body coordinate system is adopted to describe our robot model. The endpoint of supporting leg is chosen as the original point, the forward direction as the positive direction of x axis, and the negative direction of gravity as the positive direction of y axis. L_1 and L_2 denote as the length of thigh and shank. α is the angle between the thigh and vertical direction. β is the angle between the shank and thigh. Moreover, α_1 and β_1 are in position direction. α_1 and β_1 denote the joint angles of supporting leg, and α_2 and β_2 are for swinging leg. Note that in this paper, we only distinguish the supporting leg and

the swinging leg but do not distinguish the left and right leg. By switching the role of swinging leg and supporting leg in turns, the robot can walk normally. The endpoint of swinging leg P can be described as:

$$\begin{bmatrix} P_x \\ P_y \end{bmatrix} = T \begin{bmatrix} L_1 \\ L_2 \end{bmatrix} \quad (1)$$

where T is:

$$\begin{bmatrix} -\sin(\alpha_1) + \sin(\alpha_2) & -\sin(\alpha_1 - \beta_1) + \sin(\alpha_2 - \beta_2) \\ \cos(\alpha_1) - \cos(\alpha_2) & \cos(\alpha_1 - \beta_1) - \cos(\alpha_2 - \beta_2) \end{bmatrix}$$

B. Base Gait

The trajectory waveform of hip and knee joint during gait cycles are periodic and can be collected from healthy individuals. According to the theory of Fourier series, all periodical signal can be decomposed into trigonometric series. Refer to [21], a simply and accuracy gait trajectory is composed of two sine functions. Here, we choose this gait as base gait, which is shown in Fig.2. The trajectory of left leg is obtained as follows:

$$\begin{cases} L_{knee} = 11.35 + 23.69\sin(2\pi t + 1.02) \\ \quad + 11.35 + 18.54\sin(4\pi t + 0.41) \\ L_{hip} = 3.76 + 12.94\sin(2\pi t - 0.29) \\ \quad + 3.76 + 4.78\sin(4\pi t - 0.64) \end{cases} \quad (2)$$

We sample 100 frames from 0.89s to 1.39s, which record the swing leg from the beginning of swinging to the end of a swing. For easy explanation, we assume we sample m frames in the rest of this paper.

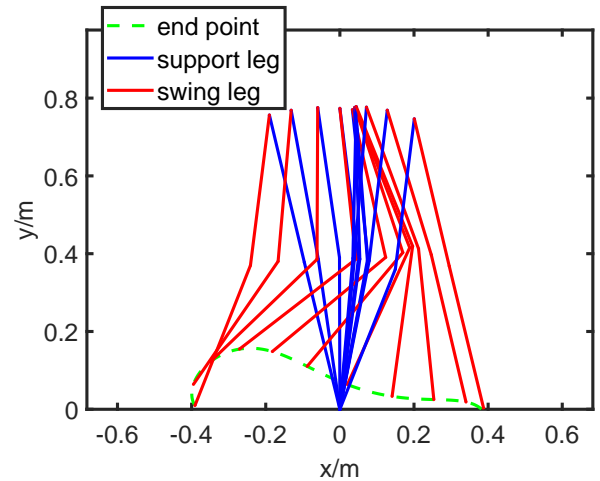


Fig. 2: Base gait.

IV. METHODOLOGY

A. Algorithm Overview

As mentioned in III-B, we sample m frames as the base gaits. Here "frame" denotes a group of all joint angles of LLE at sampling time. A frame is described as $\mathbf{z}(n) = [\alpha_1(n), \beta_1(n), \alpha_2(n), \beta_2(n)]^T$, where n denotes the n_{th} sampling in m frames. Then, from Equ.1, we can calculate point $P = [P_x, P_y]^T$ from frame \mathbf{z} . It is assumed that that:

$$P = f(\mathbf{z}) \quad (3)$$

where f denotes the mapping function frame \mathbf{z} to the coordinate of point P . Then, define the whole base gait

containing m frames as $\mathbf{Z} = \{\mathbf{z}(1), \mathbf{z}(2), \dots, \mathbf{z}(m)\}$ and the adjacent error of \mathbf{Z} as:

$$\begin{aligned} \mathbf{AE}(\mathbf{Z}) &= \{\mathbf{z}(2) - \mathbf{z}(1), \mathbf{z}(3) - \mathbf{z}(2), \dots, \mathbf{z}(m) - \mathbf{z}(m-1)\} \\ &= \{\mathbf{e}_z(1), \mathbf{e}_z(2), \dots, \mathbf{e}_z(m-1)\} \end{aligned} \quad (4)$$

where $\mathbf{e}_z(n)$ denotes the error between two adjacent frame $\mathbf{z}(n)$ and $\mathbf{z}(n+1)$ in base gait. At each frame i the end point P is denote as $P(i) = [P_x(i), P_y(i)]^T$. Then, we can build a graph whose node is the frames \mathbf{z} and the weak edges among nodes are the adjacent errors \mathbf{e} , which is quite similar to the pose graph. Here this kind of edges is called **“residual edge”**.

Furthermore, we need to generate variable gaits to step over obstacles and adjust the stride through solving the graph. For these proposes, some **“obstacle edges”** are added to measure the relative pose between the endpoint of swing leg and obstacles into the graph. Then, we add a **“end edge”** into the graph, which measures the distance between endpoint P in the last frame of one gait and the target foothold. The overview of the graph is shown in Fig.1

Note that the proposed algorithm is the inverse process of the PGO. The PGO is trying to eliminate the estimation error between adjacent frames to eliminate the resulting error while GGO is trying to add little error into every frame to generate a totally different gait.

B. Residual Edge

It is assumed that the generate gaits also contains m frames, the n_{th} frame in generated gait is $\mathbf{g}(n)$ and the residual error between two adjacent frames is $\mathbf{e}_g(n)$. The generated gait is $\mathbf{G} = [\mathbf{g}(1), \mathbf{g}(2), \dots, \mathbf{g}(m)]$. With residual edge, the difference between generate gaits and base gait will be well-proportioned propagated to all frames. Hence, if we only compare one residual error between two adjacent frames $\mathbf{e}_g(n)$ and $\mathbf{e}_z(n)$ in both generated gaits and base gait, they will be quite similar. Thus the comfort of generated gait can be guaranteed. When walking with both generated gaits and base gait, patients won't feel quite different from frame n to $n+1$. Then, define the residual edges as a minimization problem:

$$\min_{\mathbf{G}} \sum_{i=1}^{m-1} \|(\mathbf{g}(i+1) - \mathbf{g}(i)) - (\mathbf{z}(i+1) - \mathbf{z}(i))\|^2 \quad (5)$$

Note that the angle of the knee can not be negative as a negative angle may hurt patients. Such that we add a constraint into Equ.5 to ensure β_1 and β_2 stay positive. Then, the modified minimization problem can be written as:

$$\min_{\mathbf{G}} \sum_{i=1}^{m-1} \{ \|\mathbf{e}_g(i) - \mathbf{e}_z(i)\|^2 + \lambda \sum_{j=1}^2 ReLU(-\beta_j) \} \quad (6)$$

where λ is a gain of the constraint on knee's angle to ensure the second term in Equ.6 can generate enough gradient. $ReLU$ is a activation function that often used in deep learning:

$$ReLU(x) = \begin{cases} x, & \text{if } x > 0 \\ 0, & \text{if } x \leq 0 \end{cases} \quad (7)$$

With $ReLU$, positive β_1 and β_2 won't make any influence to this graph, while negative will generate gradient.

C. Obstacle Edge

The obstacle edge is added into the graph to help LLE robot to step over a obstacle object as shown in Fig.1. By adopting the AABB bounding box of obstacles, we can always regard the obstacles as rectangle. It is assumed that a obstacle object is located at the range of $[x_s, x_e]$ and the height of obstacle is h . Then, the obstacle avoidance problem can be simplified as:

$$P_y(i) > h, \forall i, P_x(i) \in [x_s, x_e] \quad (8)$$

Assumed $\mathbf{O} = \{\mathbf{g}(i), \mathbf{g}(i+1), \dots, \mathbf{g}(j)\}$ as a gather of all frames in a generate gait whose P_x is in $[x_s, x_e]$, the obstacle edge can be written as:

$$\min_{\mathbf{O}} \sum_{k=i}^j \|exp(\gamma \cdot ReLU(h + \delta - P_y(k))) - 1\|^2 \quad (9)$$

where δ is a hyper-parameters to strengthen the robustness of our algorithm. Note that we only optimize the frames in \mathbf{O} . $ReLU(h + \delta - P_y(k))$ indicate that only when $P_y(k) < h + \delta$, the frame $\mathbf{g}(k)$ will be optimized. γ is a gain to enlarge the error. Besides, we apply a exp activation function on the error. As shown in Fig.3, when x grows, $exp(ReLU(x))$ grows rapidly. As the frames that take part in obstacle edge are much fewer than that in residual edge, such that the active function can ensure the obstacle edge provide enough gradient to ensure the gait can step over the the obstacle.

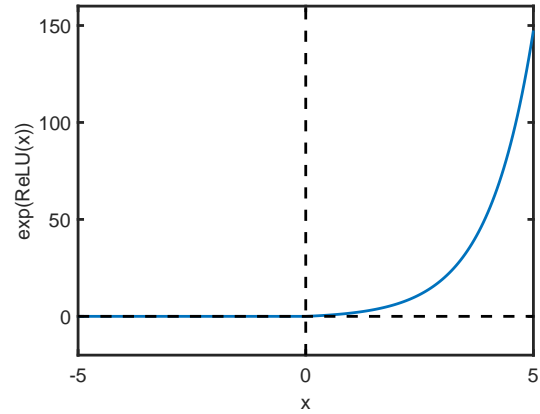


Fig. 3: The function $exp(ReLU(x))$.

D. End Edge

The end edge only influences the last frame of generated gaits. End edge is adopt to set a proper foothold of the swing leg. It can be used for stride adjustment or stair ascent and descent. Now we set a target foothold for the swing leg as $F = [F_x, F_y]^T$. Thus, the end edge can be denote as Equ.10, where ω is the gain of end edge and $\mathbf{g}(m)$ is the last frame of the gait.

$$\min\{\omega \|f(\mathbf{g}(m)) - F\|^2\} \quad (10)$$

The angle between ground and shank of LLE when swing leg reach the foothold should also be considered. For example, when a healthy person ascends one stair, his swing leg is approximately perpendicular to the ground in most cases. This found drives us to add a term to constrain the angle

between ground and shank of swing leg in last frame. Now we assume the angle as ϵ . The ϵ can be calculated by:

$$\epsilon = \alpha_2(m) - \beta_2(m) \quad (11)$$

where $\alpha_2(m)$ and $\beta_2(m)$ are the value of α and β in the last frame of generated gait. Denoting the target angle as ϵ_t , then the full end edge can be written as:

$$\min\{\omega(\|f(\mathbf{g}(m)) - F\|^2 + \|\epsilon - \epsilon_t\|)\} \quad (12)$$

E. Solving The Graph

Adding all the edges mentioned in IV-B, IV-C and IV-D, we can build a full graph for GGO algorithm. Then, solving the gait graph is equal to solve a minimization problem, as shown in Equ.13. Based on different application, edges can be added or removed from the graph. By using the non-linear optimization algorithm like L-M or DogLeg, the graph can be solved.

$$\min_{\mathbf{G}} \left\{ \begin{array}{l} \sum_{i \in \mathbf{G}} \{ \|\mathbf{e}_g(i) - \mathbf{e}_z(i)\|^2 \\ + \lambda \sum_{j=1}^2 \text{ReLU}(-\beta_j) \} + \\ \sum_{k \in \mathbf{O}} \{ \exp(\gamma \cdot \text{ReLU} \\ (h + \delta - f(\mathbf{g}(i)))) - 1 \|^2 \} + \\ \omega(\|f(\mathbf{g}(m)) - F\|^2 + \|\epsilon - \epsilon_t\|) \} \end{array} \right. \quad (13)$$

V. EXPERIMENT

In this section, we will show various applications of GGO on the LLE robot in both simulations and experiments. These applications contain three parts. 1) Generation of gaits with different strides. 2) Generation of gaits for dimensions obstacles avoidance. 3) Generation of gaits for stair ascent and descent. All these gaits are generated from one base gait introduced in Fig.2. All graphs are solved by Ceres Solver[22], and the non-linear optimization algorithm is chosen as DogLeg. And $L_1 = L_2 = 0.39(m)$ in this section.

A. Generate Gaits with Different Strides

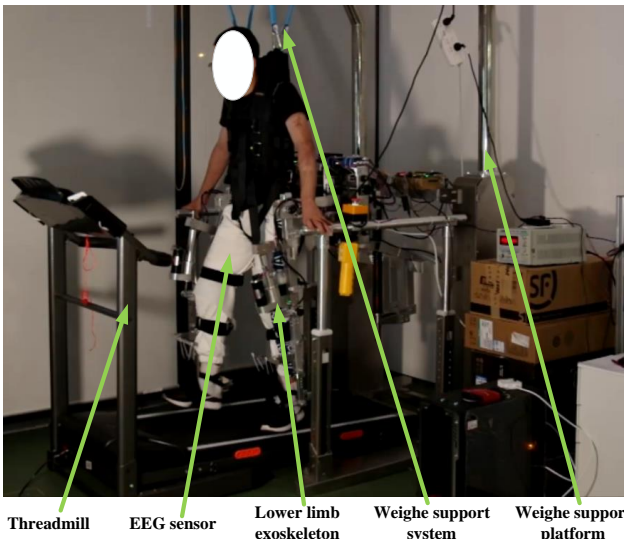


Fig. 4: Experimental platform.

Define the stride as the distance between point P in the first frame and point P the last frame in one gait. The stride of base gait is $0.78(m)$. Now we show how to generate a

gait with stride of $0.975(m)$. Here, only "residual edge" and "end edge" should be added into the graph and we won't add the constraint of the angle between shank and ground into the "end edge". The hyper-parameters is set to $\lambda = 5, \omega = 5$. Then, we can generate a gait with stride of $0.975(m)$ in two steps:

- **First**, initialize \mathbf{G} with \mathbf{Z} , and set the target foothold of swing leg to $F = [0.4875, 0]^T(m)$. Then, build the graph and solve the graph by DogLeg algorithm.
- **Second**, define the gait generate by first step as \mathbf{G}^1 and the last frame of \mathbf{G}^1 as $\mathbf{g}^1(m)$. Then, initialize all frames in \mathbf{G} as \mathbf{g}_m^1 and also set $F = [0.4875, 0]^T(m)$. Finally, build the graph and solve the graph by DogLeg algorithm.

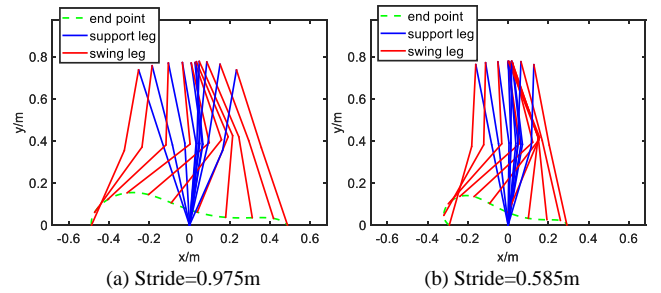


Fig. 5: Generated gait with different stride.

Note that there exists a role switching of support leg and swing leg in the two steps. With the same process, we can generate a gait with a stride of $0.585(m)$. The gaits with stride of $0.975(m)$ and $0.585(m)$ are shown in Fig.5(a) and Fig.5(b).

To verify the effectiveness of the proposed algorithm for the real LLE robot, we designed an experiment. Our experimental platform is shown in Fig.4. The lower limb rehabilitation robotic system consists of a treadmill, a weight support platform, and a lower limb exoskeleton. By detecting the activity degree of muscle in thigh using an EEG sensor, the gait stride of $0.975(m), 0.78(m)$ and $0.585(m)$ would switch autonomously. The higher activity degree project to longer stride. The trajectory of each joint in generated gait is shown in Fig.6(a) and the residual error of every frame is shown in Fig.6(b). From Fig.6(a), the generated gait is smooth enough to be tracked and quite similar to base gait. From Fig.6(b), It is found that the huge different strides in the whole gaits are caused by the accumulation of the little difference in every frame. As the different of residual error among the three gaits in each frame is significantly small, the feeling of patient moving from i_{th} frame to $i + 1_{th}$ is quite similar. Thus the generated gait is also comfortable for patients when doing rehabilitation training. To analysis the difference between generated gaits and base gait, we calculate the average value of absolute joint angle error between generated gait and base gait, as shown in Tab.I. The biggest difference between the two generated gaits and base gait are the knee angle of the swing leg. However, the largest value is also smaller than 3° , such that the comfort performance of generated gaits can be guaranteed.

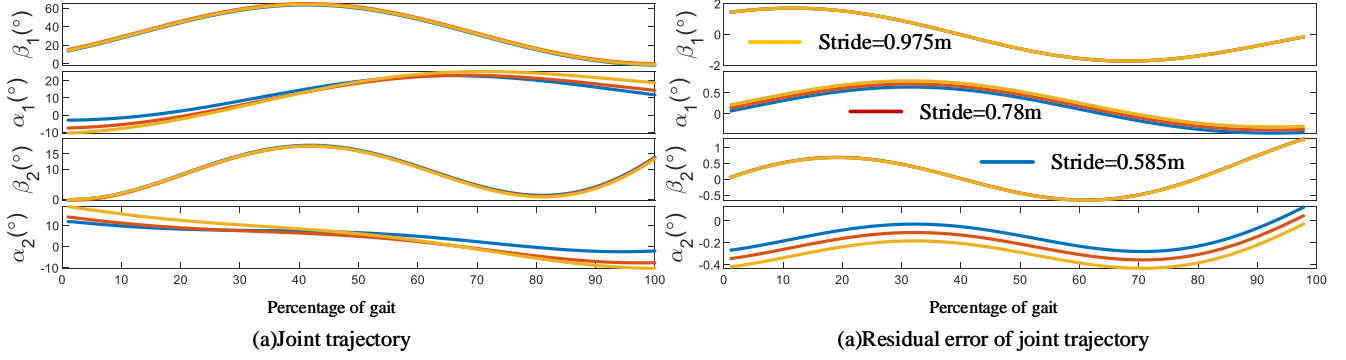


Fig. 6: Generated gait for stir descents.

TABLE I: The average absolute error between generated gait and base gait

Joint	β_1°	α_1°	β_2°	α_2°
Stride=0.585(m)	1.4508	1.9439	0.2686	2.3270
Stride=0.975(m)	0.7991	1.9386	0.1575	2.1009

B. Generate Gaits for Obstacle Avoidance

First, we provide an example to generate a gait to step over a rectangle obstacle start from $[0.2, 0]^T(m)$ to $[0.25, 0.8]^T(m)$ as shown in Fig.7. We add all the three types of edges into the graph. Specifically, we do not add the constraint of the angle between shank and ground into the "end edge". The hyper-parameters of the graph is set to $\lambda = 5, \omega = 5m, \gamma = 4, \delta = 0.02$, and the target foothold of swing leg is $F = [0.39, 0]^T(m)$. The gather \mathbf{O} contains all frame whose P_x in the range of $[0.18, 0.22](m)$. Then by using DogLeg to solve the graph, the generated gait is shown in Fig.7(a).

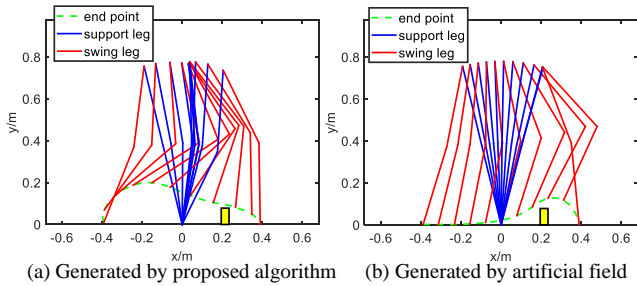


Fig. 7: The gait with different strides.

As a comparison, we generate another gait using the artificial filed algorithm [23]. The trajectory of endpoint P is generated using the artificial filed algorithm, and the joint angles calculate the joint angle in all frames by solving the inverse kinematics. The joint trajectory and residual of joint trajectory are shown in Fig.8(a) and Fig.8(b). Fig.8 shows that the gait generated by GGO much more smooth than the gait generated by AF. The great performance of CGO is because of the introduction of the residual edge. With the residual edge, the base gait plays as a teacher to guide the generation of new gait, such that the generated gait is similar to base gait. Moreover, we tried to conduct an ablation study

to demonstrate the influence of residual edge. However, the experimental results show that GGO can not generate proper gait at all without the residual edge in the graph.

In order to compare these two algorithm further, the time cost and the comfort performance are chosen as the evaluation indicator. Comfort performance is measured based on improved ZMP. Zero moment point (ZMP) [24] is an important indicator for the balance of legged robot. When ZMP is in the support area of a robot, the robot can keep balance itself. However, when ZMP is further from the foothold, the robot gets more unbalanced. Although patients in the LLE robot can keep balance with two walking sticks, as the walking stick can enlarge the supporting area so that the ZMP can be included in the supporting area. A far distance between ZMP and foothold may cause patients uncomfortable as patients should put more power on the walking stick to keep balance. The ZMP can be given by the following equation:

$$x_{zmp} = \frac{\sum_{i=1}^n m_i \left[\left(\frac{d^2 y_i}{dt^2} + g \right) x_i - y_i \frac{d^2 x_i}{dt^2} \right]}{\sum_{i=1}^n m_i \left(\frac{d^2 y_i}{dt^2} + g \right)} \quad (14)$$

where x_{zmp} is the distance between ZMP and support point. n is the link number of robot, in our problem $n = 4$. $[x_i, y_i]^T$ is the center point of the i_{th} link, and g is the gravity constant. m_i is the mass of i_{th} link. In our experimental configuration, both the length of thigh and shank as $0.39(m)$ and both the two links weight $7(kg)$. Moreover, the torso link is not considered. The average x_{zmp} of different gait is shown in Tab.III and the time cost to solve the gait graph proposed in this paper is shown in Tab.IV. The obstacles in the two tables are shown in Tab.II.

TABLE II: The experimental configuration.

Obstacles	$x_s(m)$	$x_e(m)$	$h(m)$
obstacle 1	0.2	0.25	0.08
obstacle 2	0.2	0.25	0.15
obstacle 3	0.12	0.16	0.08
obstacle 4	0.12	0.16	0.15
obstacle 5	-0.33	-0.29	0.175

In Tab.III "Base gait" denotes the performance of base gait. "Proposed" denotes the performance of our proposed algorithm. "AF" denotes the performance of the Artificial field. In Tab.IV, "iteration" denotes the iteration cycle to solve the graph and "time cost" denotes the time cost of

the proposed algorithm. The average x_{zmp} of gait generate by the artificial field algorithm is significantly higher than the gaits generated by the proposed algorithm. In addition, from Tab.IV, we found that the time cost of solving gaits for different obstacles are similar to each other, and the average time cost is 77.9ms.

TABLE III: Average x_{zmp} of different gaits.

Average $x_{zmp}(m)$	Base gait	Proposed	AF
obstacle 1	0.0828	0.0986	0.2188
obstacle 2	0.0828	0.1204	0.2382
obstacle 3	0.0828	0.0914	0.1752
obstacle 4	0.0828	0.1460	0.1969
obstacle 5	0.0828	0.0823	0.2515
Average	0.0828	0.0828	0.2162

TABLE IV: Time cost of proposed algorithm

	Iterations	Time Cost(ms)
obstacle 1	47	77.6
obstacle 2	47	77.3
obstacle 3	44	76.8
obstacle 4	50	80.9
obstacle 5	35	76.9
Average	44.6	77.9

C. Generate Gaits for Stair Ascent and Descent

We firstly provide an example to generate a gait for stair ascent. In this example, the stair has two stages, and the rising edges are at $x = 0.29(m)$ and $x = 0.68(m)$. The height of both stairs is $0.1(m)$. The generated gait is shown in Fig.9, $t = n\%$ denotes the frame is sampling from the $n\%$ time of the whole gait. To generate the gait shown in Fig.9, we add all three kinds of edges into the graph. The hyper-parameters are set to $\lambda = 5, \omega = 5, \gamma = 4, \delta = 0.02$ and the target angle $\epsilon_t = 90^\circ$. Then, we can generate the gait within two steps:

- **First**, initialize \mathbf{G} with \mathbf{Z} , and set the target foothold of swing leg to $F = [0.39, 0.1]^T(m)$. Then, set the gather \mathbf{O} contains all frame whose P_x is in the range of $[0.28, 0.30](m)$, and set the height of obstacle to $h = 0.1(m)$. Finally, build the graph and solve the graph by the DogLeg algorithm. Here we can generate the gait to step over the first stage, which is shown in the first row of Fig.9.
- **Second**, define the gait generate by first step as \mathbf{G}^1 and the last frame of \mathbf{G}^1 as \mathbf{g}_m^1 . Then, initialize all frames in \mathbf{G} as \mathbf{g}_m^1 . Note that the original point is always set to the endpoint of the supporting leg. The supporting leg and swing leg has changed after the first step. Then, set the rest of the configuration the same as the first step. We can generate the second step to step over the second stage, which is shown in the second row of Fig.9.

As mentioned in V-A, there exists a roles switch of support leg and swing leg in the two steps. In a similar way, a gait for stair descent can be generated by changing the foothold to $F = [0.39, -0.1]^T(m)$. the results are shown in Fig.10.

To verify the effectiveness of the algorithm in the real LLE robot, we designed an experiment. Our experimental platform is shown in Fig.11. We adopt a Microsoft Kinect2

to detect the stair model. Note that the real LLE is a bit little different from the model in Fig.1. The endpoint of swing leg shown in Fig.1 is actually the ankle joint in real robot shown in Fig.11. We assume that the feet are always parallel with the ground. In Fig.11, P_f^s denotes the point of intersection between vertical line from point P to feet of swing leg, P_t^s denotes the tiptoe of swing leg. We aim to generate a trajectory for the point P to make sure the exoskeleton robot can step over the stair and no collisions occur among P_f^s , P_t^s and stairs. Such that the stair in real-world which starts from $x = x_{stair}$ and with height of $h = h_{height}$ is equivalent to be a stair start from $x = x_{stair} - L_f$ and with height of $h = h_{height} + L_a$ for point P as shown in Fig.12. Note that the stair model detected by Kinect is also transformed to the body coordinate system whose original point is the ankle point of supporting leg. For safety consideration, we do not generate gaits for stair ascent from Fig.2. We collect a gait trajectory from a healthy person for stair ascent, as shown in Fig.13. In this gait, one cycle of stair ascent contains two steps, the first step start from $\alpha_1 = \alpha_2 = \beta_1 = \beta_2 = 0$ as shown in Fig.13(a) and the second step end with $\alpha_1 = \alpha_2 = \beta_1 = \beta_2 = 0$ as shown in Fig.13(b).

The height of the stair for gait trajectory collection is $0.12m$, and the foothold for the point P is $[0.25, 0.12]^T(m)$. In the experimental configuration, the height of the stair is $0.06m$, so we set the foothold of point p to $[0.27, 0.06]^T(m)$. The experimental results are shown in Fig.14 and Fig.15. As shown in Fig.14, the two curves are the trajectory of point P of base gait and generated gait. The joint trajectory of both legs is shown in Fig.15, the four subgraphs are the angle of the hip joint of the right leg, the angle of knee joint of the right leg, the angle of hip joint of the left leg and the angle of knee joint of the left leg. This result demonstrates that our approach can be extended to generate gait for stair ascent and descent. Moreover, the generated gaits are functional and comfortable.

VI. CONCLUSION & FUTURE WORK

In this paper, we propose a graph-based algorithm to generate variable gaits from one base gait for stride adjustment, obstacle avoidance and stair ascent and descent. We show the generalization performance for different applications and usability by conducting a large number of simulations and experiments. Moreover, we show the superior performance by comparing against other algorithms using for mobile robots. We open source the C++ implementation to benefit the community.

Although the proposed algorithm works well in variants applications, there are still many directions to perfect our research in the future. The collision problem, including collision volume should be considered in a more precise way, which is simplified in this paper. Besides, the strategy for choosing the foothold of the swinging leg should also be carefully designed.

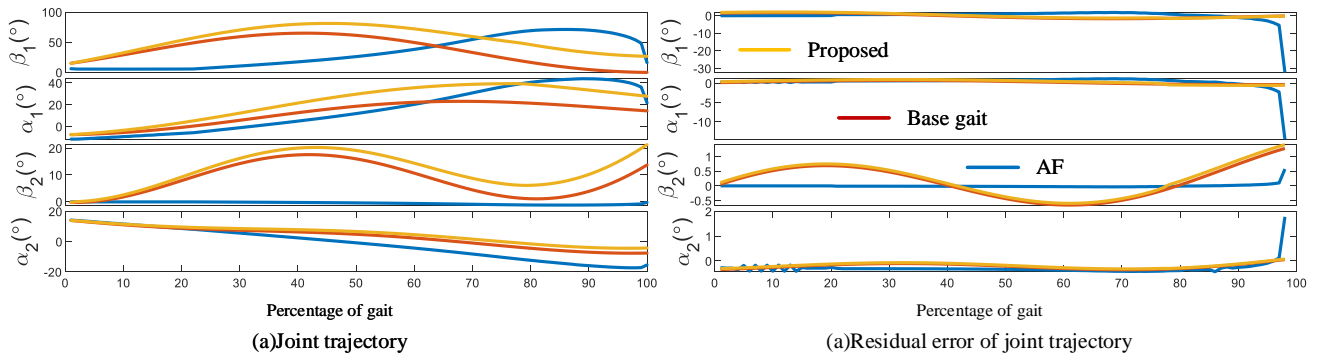


Fig. 8: Generated gait for stir descents.

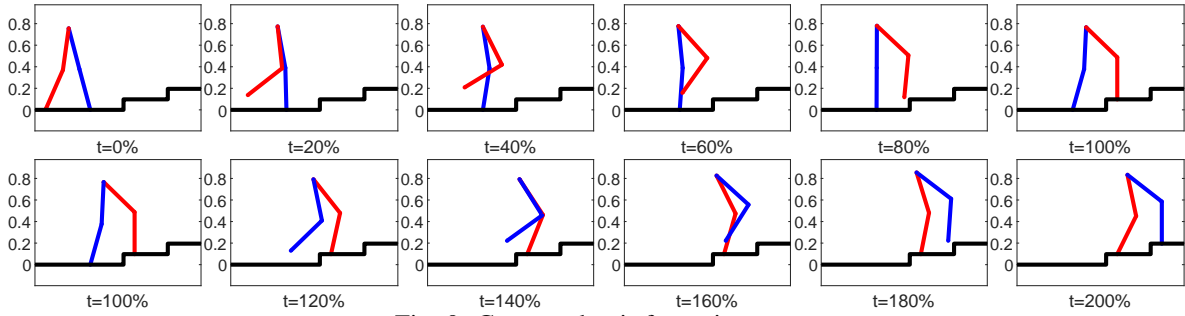


Fig. 9: Generated gait for stair ascents.

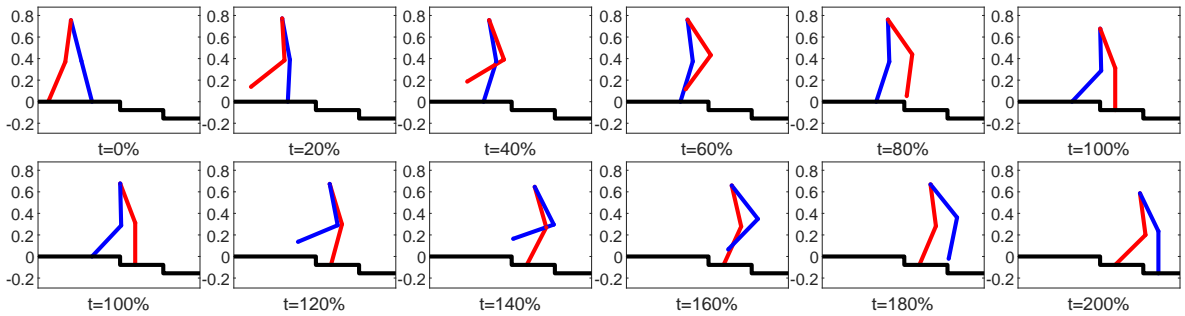


Fig. 10: Generated gait for stir descents.

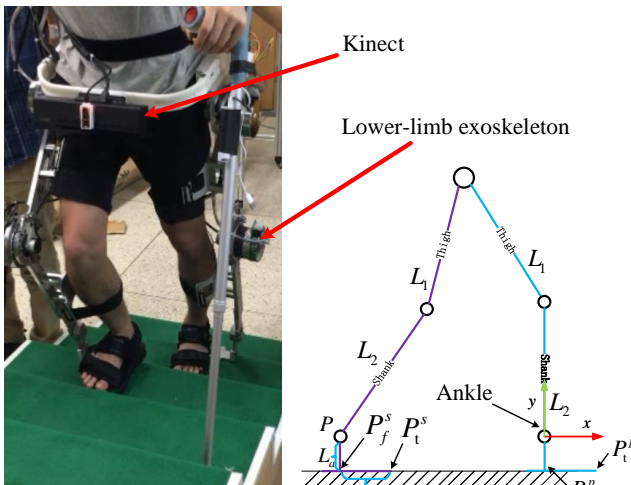


Fig. 11: Experimental robot for stair ascent.

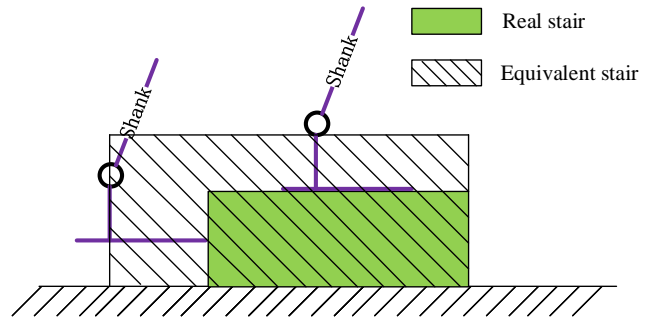


Fig. 12: Equivalent stair for point P .

REFERENCES

- [1] L. Wuli, O. Jianjun, Y. Zenghui *et al.*, "Thinking and methods of acupuncture treatment for spasm and paralysis after apoplexy [j].", *Chinese Acupuncture & Moxibustion*, vol. 6, 2003.
- [2] H. Kazerooni, "Exoskeletons for human power augmentation," in 2005

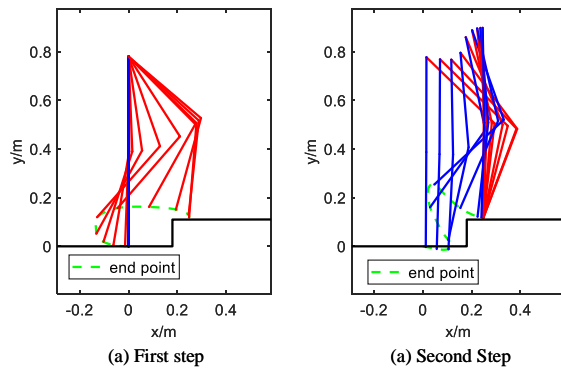


Fig. 13: Collected gait for stair ascent.

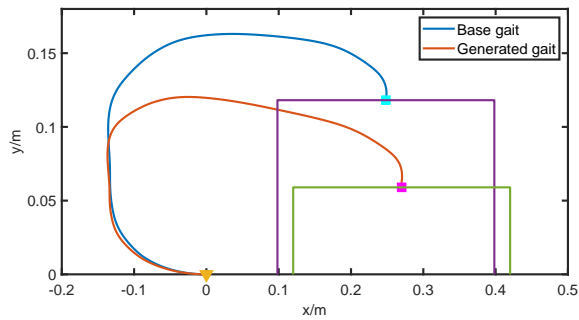


Fig. 14: Equivalent stair for point P .

IEEE/RSJ International conference on intelligent Robots and Systems. IEEE, 2005, pp. 3459–3464.

- [3] S. A. Murray, K. H. Ha, C. Hartigan, and M. Goldfarb, “An assistive control approach for a lower-limb exoskeleton to facilitate recovery of walking following stroke,” *IEEE Transactions on Neural Systems and Rehabilitation Engineering*, vol. 23, no. 3, pp. 441–449, 2014.
- [4] G. Zeilig, H. Weingarden, M. Zwickler, I. Dudkiewicz, A. Bloch, and A. Esquenazi, “Safety and tolerance of the rewalk exoskeleton suit for ambulation by people with complete spinal cord injury: a pilot study,” *The journal of spinal cord medicine*, vol. 35, no. 2, pp. 96–101, 2012.
- [5] H. Kawamoto and Y. Sankai, “Power assist method based on phase sequence and muscle force condition for hal,” *Advanced Robotics*, vol. 19, no. 7, pp. 717–734, 2005.
- [6] S. Tanabe, E. Saitoh, S. Hirano, M. Katoh, T. Takemitsu, A. Uno, Y. Shimizu, Y. Muraoka, and T. Suzuki, “Design of the wearable power-assist locomotor (wpa) for paraplegic gait reconstruction,” *Disability and Rehabilitation: Assistive Technology*, vol. 8, no. 1, pp. 84–91, 2013.
- [7] J. Sergey, S. Sergei, and Y. Andrey, “Study of controlled motion of an exoskeleton performing obstacle avoidance during a single support walking phase,” in *2016 20th International Conference on System Theory, Control and Computing (ICSTCC)*. IEEE, 2016, pp. 113–118.
- [8] S. Jatsun, S. Savin, and A. Yatsun, “Footstep planner algorithm for a lower limb exoskeleton climbing stairs,” in *International Conference on Interactive Collaborative Robotics*. Springer, 2017, pp. 75–82.
- [9] A. K. Raj, P. D. Neuhau, A. M. Moucheboeuf, J. H. Noorden, and D. V. Lecoutre, “Mina: a sensorimotor robotic orthosis for mobility assistance,” *Journal of Robotics*, vol. 2011, 2011.
- [10] H. Hoffmann, P. Pastor, D.-H. Park, and S. Schaal, “Biologically-inspired dynamical systems for movement generation: automatic real-time goal adaptation and obstacle avoidance,” in *2009 IEEE International Conference on Robotics and Automation*. IEEE, 2009, pp. 2587–2592.
- [11] D.-H. Park, H. Hoffmann, P. Pastor, and S. Schaal, “Movement reproduction and obstacle avoidance with dynamic movement primitives and potential fields,” in *Humanoids 2008-8th IEEE-RAS International Conference on Humanoid Robots*. IEEE, 2008, pp. 91–98.
- [12] H. Zhao, M. Powell, and A. Ames, “Human-inspired motion primitives and transitions for bipedal robotic locomotion in diverse terrain,”

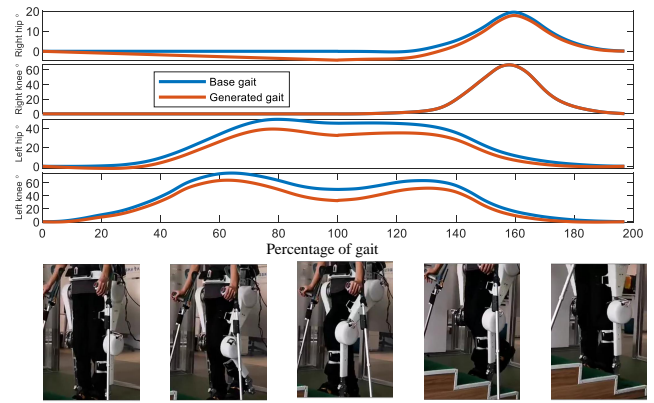


Fig. 15: Equivalent stair for point P .

Optimal Control Applications and Methods, vol. 35, no. 6, pp. 730–755, 2014.

- [13] M. J. Powell, H. Zhao, and A. D. Ames, “Motion primitives for human-inspired bipedal robotic locomotion: walking and stair climbing,” in *2012 IEEE International Conference on Robotics and Automation*. IEEE, 2012, pp. 543–549.
- [14] A. Ekelem, S. Murray, and M. Goldfarb, “Preliminary assessment of variable geometry stair ascent and descent with a powered lower limb orthosis for individuals with paraplegia,” in *2015 37th Annual International Conference of the IEEE Engineering in Medicine and Biology Society (EMBC)*. IEEE, 2015, pp. 4671–4674.
- [15] T. Taketomi and Y. Sankai, “Stair ascent assistance for cerebral palsy with robot suit hal,” in *2012 IEEE/SICE International Symposium on System Integration (SII)*. IEEE, 2012, pp. 331–336.
- [16] C.-H. Zhong, X. Zhao, F.-Y. Liang, H. Ma, and W.-H. Liao, “Motion adaption and trajectory generation of stair ascent and descent with a lower limb exoskeleton for paraplegics,” in *2019 IEEE/ASME International Conference on Advanced Intelligent Mechatronics (AIM)*. IEEE, 2019, pp. 612–617.
- [17] Y. Cong, X. Li, J. Liu, and Y. Tang, “A stairway detection algorithm based on vision for ugv stair climbing,” in *2008 IEEE International Conference on Networking, Sensing and Control*. IEEE, 2008, pp. 1806–1811.
- [18] C. Zhong, Y. Zhuang, and W. Wang, “Stairway detection using gabor filter and fppg,” in *2011 International Conference of Soft Computing and Pattern Recognition (SoCPar)*. IEEE, 2011, pp. 578–582.
- [19] M. Bansal, B. Southall, B. Matej, J. Eledath, and H. Sawhney, “Lidar-based door and stair detection from a mobile robot,” in *Unmanned Systems Technology XII*, vol. 7692. International Society for Optics and Photonics, 2010, p. 769203.
- [20] L. Carlone, R. Tron, K. Daniilidis, and F. Dellaert, “Initialization techniques for 3d slam: a survey on rotation estimation and its use in pose graph optimization,” in *2015 IEEE international conference on robotics and automation (ICRA)*. IEEE, 2015, pp. 4597–4604.
- [21] K. Gui, H. Liu, and D. Zhang, “Towards multimodal human-robot interaction to enhance active participation of users in gait rehabilitation,” *IEEE Transactions on Neural Systems & Rehabilitation Engineering*, pp. 1–1.
- [22] S. Agarwal, K. Mierle *et al.*, “Ceres solver,” 2012.
- [23] M. C. Lee and M. G. Park, “Artificial potential field based path planning for mobile robots using a virtual obstacle concept,” in *Proceedings 2003 IEEE/ASME International Conference on Advanced Intelligent Mechatronics (AIM 2003)*, vol. 2. IEEE, 2003, pp. 735–740.
- [24] S. Kajita, F. Kanehiro, K. Kaneko, K. Fujiwara, K. Harada, K. Yokoi, and H. Hirukawa, “Biped walking pattern generation by using preview control of zero-moment point,” in *2003 IEEE International Conference on Robotics and Automation (Cat. No. 03CH37422)*, vol. 2. IEEE, 2003, pp. 1620–1626.